CFD SIMULATION OF FORTUM PTS EXPERIMENT

Timo Toppila
Fortum Nuclear Services, Finland

Abstract

Detailed simulation of the thermal stresses of the reactor pressure vessel (RPV) wall in case of pressurized thermal shock (PTS) requires the simulation of the thermal mixing of cold high-pressure safety injection (HPI) water injected to the cold leg and flowing further to the downcomer. The simulation of the complex mixing phenomena including e.g. stratification in the cold leg and buoyancy driven plume in the downcomer is a great challenge for CFD methods and requires careful validation of the used modelling methods.

The selected experiment of Fortum mixing test facility modelling the Loviisa VVER-440 NPP has been used for the validation of CFD methods for thermal mixing phenomena related to PTS. The experimental data includes local temperature values measured in the cold leg and downcomer. Conclusions have been made on the applicability of used CFD method to thermal mixing simulations in case with stratification in the cold leg and buoyant plume in the downcomer.

Introduction

Pressurized thermal shock (PTS) analysis is required for VVER type nuclear power plants to certify the reactor pressure vessel (RPV) integrity. One essential part of PTS analysis is the thermal hydraulic analyses needed to produce the thermal and pressure loads affecting the RPV in case of relevant plant transients. In case of fast cool-down transients where the downcomer water rapidly cools down to the emergency core coolant system (ECCS) injection temperature, the system code calculation is generally sufficient to produce the thermal hydraulic data needed for structural analyses. However in case of non-uniform cool-down in addition to the 1-D system code a more sophisticated way to calculate the complex flow field having for example stratification of the ECCS water in the cold legs is needed. While the most used methods nowadays are quasi 3-D methods applied in mixing codes based on engineering models or regional mixing models, the continuous increase in computation capacity is made the computational fluid dynamics (CFD) methods a promising tool for the detailed mixing simulations. [1]

For reliable simulation of PTS related mixing processes the CFD methods must be validated to determine how well the CFD model, defined by the detail level of model geometry, the mesh and the used numerical and physical models can simulate the relevant physical processes and produce the needed data. The final target data of thermal hydraulic analysis is the pressure and temperature fields on structures needed as an input for structural analysis. The CFD model should be able to model the complex mixing and stratification processes in the cold legs and the downcomer of the pressure vessel as well as the heat transfer between fluid and structures accurately enough to reproduce this data. The goal of this work is to validate the CFD model for the mixing part of the problem, so that the effect of heat transfer between structures and fluid is not yet taken into account. While this validation do not give universal tool for the PTS mixing and heat transfer simulation, it gives confidence to use the CFD modeling as a part of thermal hydraulic analysis, for example to estimate the stratification in the cold legs and downcomer and the interaction of cold ECCS water plumes in the downcomer.

A selected Fortum PTS mixing experiment is simulated using commercial CFD code FLUENT. The selected experiment has stagnant cold leg flows, and the cold high pressure injection (HPI) from the bottom of one of the cold legs. Based on the experiment the stratification in the cold leg and the density driven plume in the downcomer are expected. The target values used for the comparison are the time history of the backflow rate from the downcomer to the cold leg having the HPI nozzle and the average HPI water concentrations at the thermocouple (TC) locations at the selected levels in the downcomer near the RPV wall. Simulation errors due to the numerical methods, discretization and convergence are tried to get small enough to give an idea how accurately the physical processes are modeled by the CFD method. However the application for real scale NPP PTS simulations are kept in mind and the mesh cell and time step sizes are kept in realistic scale considering that.

The considered experiment has been simulated before in EU's 5th framework project FLOMIX-R [2]. The CFD simulations with considerably coarser mesh than used in this work produce qualitatively good results, the global flow structures and trends were reproduced fairly well. However the numerical accuracy could not be fully assured that motivated new simulations presented here.

Fortum PTS mixing experiments

The Fortum PTS mixing test facility was constructed in 1983 to study thermal mixing of cold HPI water with hot primary coolant in the Loviisa VVER-440 reactor [3]. The experimental facility consisted of a 2/5-scale model of three cold legs, downcomer and the lower plenum of reactor. The

cold HPI water was injected from the bottom of the middle one of the cold legs. The schematic figure and photo of the test facility are presented in Figure 1.

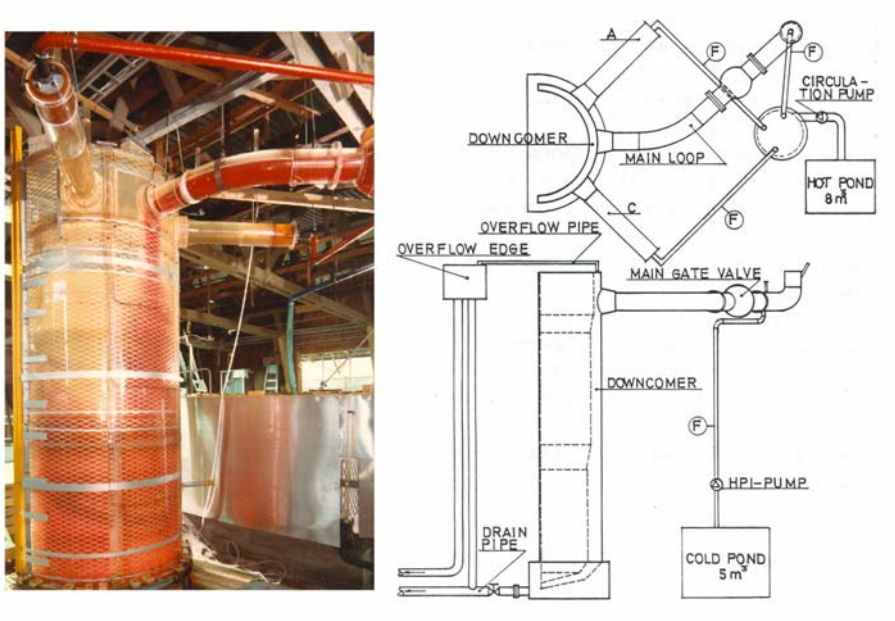

Figure 1. Fortum PTS mixing test facility

The varied parameters in experiments were the cold leg loop flow rates Q_{CL} , HPI injection flow rate Q_{HPI} and the density difference ratio between HPI injection water and water inside cold leg and downcomer $\Delta\rho/\rho$. The original experimental program consisted of about 50 tests. For this work a test with stagnant cold leg flows Q_{CL} = 0, HPI flow of Q_{HPI} = 2.31 dm^3/s and a relatively high density difference of $\Delta\rho/\rho$ = 0.16 was chosen. The total time of the measurement was 648 s with 400 measurements per thermocouple.

The mixing of the cold HPI water having a temperature of about 10 °C with the hot main fluid having a temperature of about 75 °C was measured using total of 50 thermocouples, of which nine located in the cold leg for the estimation of stratification, 27 located at the pressure vessel wall and 14 at the core barrel wall. The map of the thermocouple locations is presented in Figure 2. In the experiment an additional density difference was induced using salt ($CaCl_2$).

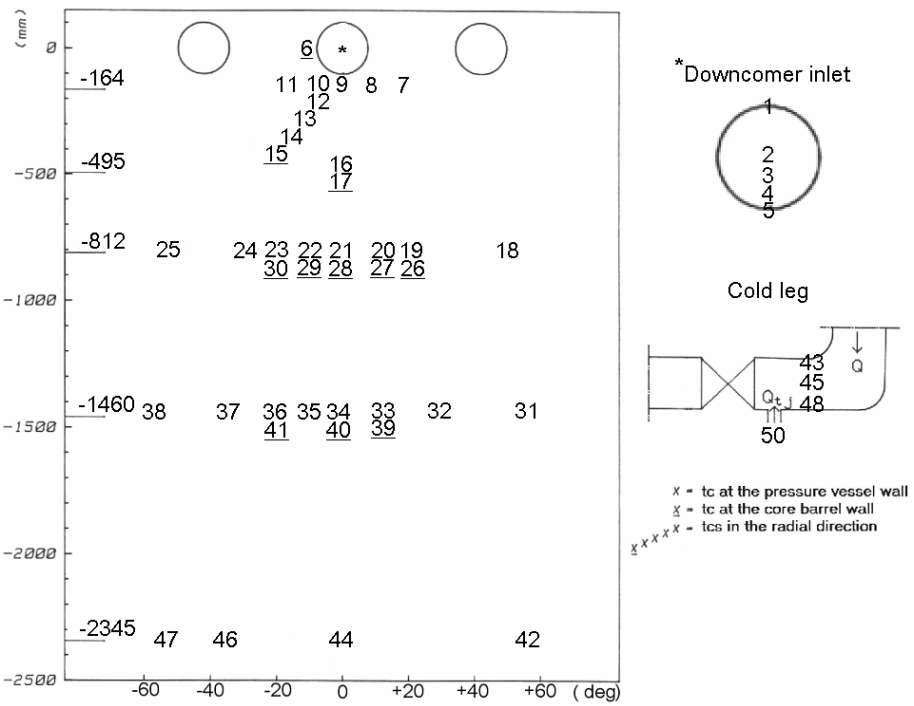

Figure 2. Thermocouple locations

CFD model of the PTS mixing test facility

The design basis for the CFD model construction was to generate model capable to reproduce the relevant flow features affecting to the mixing in PTS test but having resolution that still leaves the model adaptation to real scale NPP possible. The numerical error was tried to get so small that differences between experiment and simulation would be essentially due to the defects of the physical models or uncertainties with boundary conditions. The numerical errors were identified and handled based on the previous simulations of same experiment [2] and using recommendations of available best practice guidelines [4,5] and code manual [6].

The flow field characteristics were estimated before the construction of CFD model. The high values of Reynolds number (Re ~ 10^5) and Rayleigh number (Ra > 10^{10}) indicated turbulent flow both in the cold leg and in the vicinity of buoyant plume. The geometry and mesh of the CFD model were made using commercial pre-processor GAMBIT version 2.2.30 and simulations were made using commercial CFD code FLUENT versions 6.2.16 and 6.3.13 beta [6].

Geometry and boundary conditions

The main RPV downcomer part of the test facility, cold legs including a valve model in the cold leg with HPI injection, and the outflow chamber with the outflow pipe were included to the CFD model. The inlet boundary was defined in the HPI water pipe at about 1 m from the cold leg junction. The outflow boundary was defined in the outflow pipe at the bottom of the test facility about 1 m from the outflow chamber. The perforated bottom plate in the lower plenum was not modelled in detail but

using porous model with pressure loss term in momentum equation. Preliminary studies showed that the effect of perforated plate is small in these simulations.

The boundary conditions given for the inlet boundary were constant flow velocity corresponding specified volumetric flow rate, turbulence intensity I = 1% and turbulence length scale l = 1 mm, and the mass fraction of HPI water c_{inlet} = 1.00. A constant static pressure was specified at the outlet boundary p_{outlet} = 0.0 Pa.

The boundary condition at wall boundaries was given using FLUENT's "enhanced wall treatment" because it was assumed that y^+ would vary considerably in different areas of model. "Enhanced wall treatment" means in this case the use of law-of-the-wall function for velocity that is blended from laminar and turbulent wall functions based on the blending function of y^+ [6].

Mesh

The computation mesh was made using body-fitted block-structured mesh with hexahedral cells. The mesh size near the wall boundaries were chosen based on the y^+ values that were about 20-40 in cold leg with injection and about 60-100 in the downcomer in the vicinity of the plume. The number of cells in radial direction of downcomer was 20 giving average cell size of 2-5 mm in radial direction. The total number of cells in the computation mesh was about 800000. The mesh is presented in Figure 3.

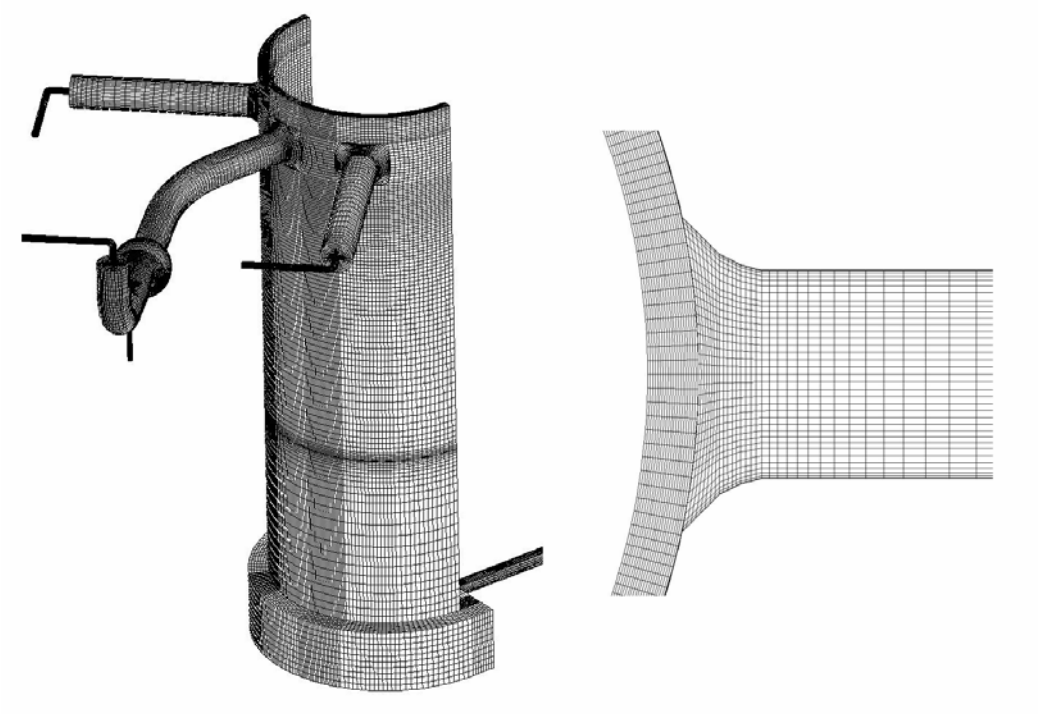

Figure 3. Computation mesh. General view (left) and the mesh at the cold leg and downcomer junction (right)

Material properties

The density difference between the HPI water and the initial cold leg water in mixing tests was due to the combined effect of temperature difference and added salt. The CFD simulation included two fluids with different densities, and the local mixture density was calculated as a volume fraction weighted average. The viscosity of mixture was defined based on the function of temperature in experiment. The (molecular) mass diffusivity D was neglected based on assumption that mixing is dominated by turbulent mixing process, and a very small value of 10^{-10} m^2/s was used.

Physical models

The conservation equations for mass and momentum were solved together with equations of k and ε of FLUENT's realizable k-ε turbulence model [6] and the convection-diffusion equation for mixture species transport:

$$\frac{\partial}{\partial t}(\rho c_i) + \nabla \cdot (\rho \vec{v} c_i) = \nabla \cdot \left(\left(\rho D + \frac{\mu_t}{Sc_t} \right) \nabla c_i \right) \qquad (1)$$

where c_i is the local mass faction of species i, Sc_t is the effective Schmidt number having constant value of Sc_t =0.7 and μ_t is eddy viscosity defined by used turbulence model. FLUENT's Realizable k-ε model includes extra terms in equations of k and ε for generation of k due to the buoyancy and the corresponding contribution to production of ε that were activated in simulations. With used "enhanced wall treatment" the simplified formulas for turbulence quantities at the wall adjacent cells are used. [6]

Numerical models

FLUENT's pressure-based (segregated) solver for incompressible flow was used. The numerical models used were chosen based mostly on recommendations of FLUENT manual [6]. For control-volume-based spatial discretization the upwind scheme with 2nd order accuracy was used for convective terms and central differencing for diffusion terms, for fully implicit time integration the discretization with 2nd order accuracy was used. For pressure interpolation the FLUENT's body-force-weighted scheme was used and the pressure-velocity coupling was made using SIMPLE scheme [6].

Calculations

Time period of about 200 seconds from the beginning of the total of 648 seconds experiment was simulated. Based on the experiment during this period the flow field finds a quasi-steady state with stratification in the cold leg, about a constant location of cold water plume in the downcomer and a steady temperature decrease of average fluid temperature.

The comparison with experiments was made using two target variables:

- Time history of the ratio of mass flow of hotter water flowing from downcomer to cold leg Q_h and massflow of injected HPI water Q_{HPI} to cold leg, "backflow ratio"

$$Q^* = \frac{Q_{\mathrm{h}}}{Q_{\mathrm{HPI}}} \approx \frac{1 - c_{05}}{c_{05}} \tag{2}$$

where c_{05} is the mass fraction of the HPI water at the measurement location number 05 in the bottom of the cold leg near downcomer. The backflow ratio variable tells directly about the mixing in the cold leg.

- Time-averages of HPI water mass fractions c_{ave} at measurement points at two vertical levels: $z = -821$ mm and $z = -1460$ mm:

$$c^i_{\mathrm{ave}} = \frac{\sum_j \Delta t_j c^i_j}{\sum_j \Delta t_j} \tag{3}$$

Time average tells how much specific measurement location "sees" cold HPI water during the transient, which is relevant data considering structural analysis. Considering the Loviisa NPP pressure vessel the level $z = -1460$ mm in the test facility is important because in the real pressure vessel there is a circumferential weld at the relatively same location.

Before the comparison of numerical results with experiments the numerical studies were made by re-calculating the selected parts of calculated transient to study the effect of the convergence criteria, the computation mesh and the time step size.

Numerical studies

Convergence criterion for the iteration process per time step was determined based on the comparison of integral mass error of iteration and the local concentration and velocity values. The used value of 0.01 for convergence is justified in Figures 4 and 5, from which it can be seen that the criterion gives similar enough behavior of followed local values over the comparison period of five time steps. The convergence criterion studies pointed out that criterion based on the mass error is better than the constant number of iterations per time step because there was significant differences in needed iteration number in different parts of the transient. Also the temporary poor convergence might lead to misbehaving flow field while the simulation was calculated further.

Influence of the mesh and time-step size was determined by re-calculating about 10 second part of the simulation with a denser mesh and a smaller time step size. One "coupled" test simulation was used because of the strong coupling of mesh and time step. The computation mesh was locally refined using once the FLUENT code's automatic adaptation option: the hexahedral computation cells in the cold leg and circumferentially in the middle of the downcomer were split to form eight cells from one. The total number of cells increased from about 0.8 million to about 3.8 million. Respectively the time step size was decreased to half from the initial time step: $\Delta t = 0.1$ s was changed to $\Delta t = 0.05$ s in order to maintain about the same value of CLF. The CLF was about 1 in the cold leg, about 2-8 in the vicinity of plume in the downcomer and about 1 in the other parts of the downcomer. The code manual recommends use values less than 20-40, while the value of 1 is optimal. The target variables used for comparison were the backflow ratio Q^* and the average concentration values at the TC locations at level z = −812 mm. Comparison of results indicated that finer mesh and smaller time step bring out

some new small time scale effects but the effect to target variables were negligible. The target variables compared are presented in Figure 6.

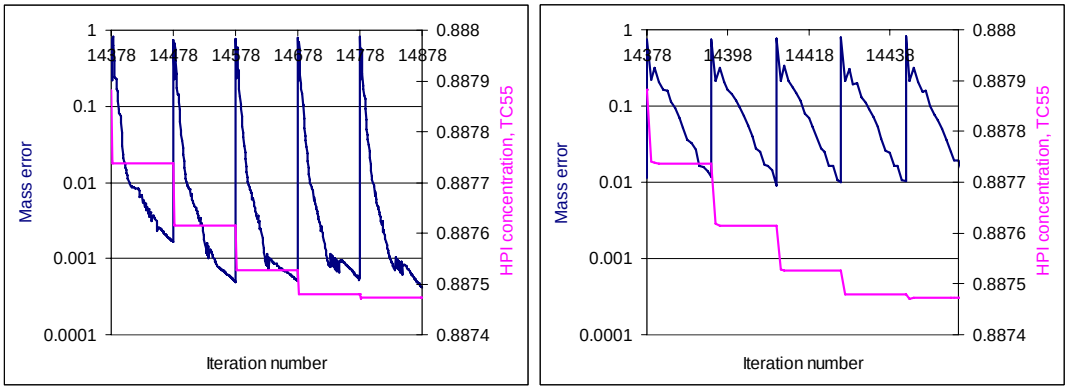

Figure 4. Effect of convergence criterion to HPI water concentration in TC55 in cold leg: 100 iterations per time step (left) compared to iteration criterion based on the total mass iteration error summed over the mesh (mass residual) < 0.01 (right).

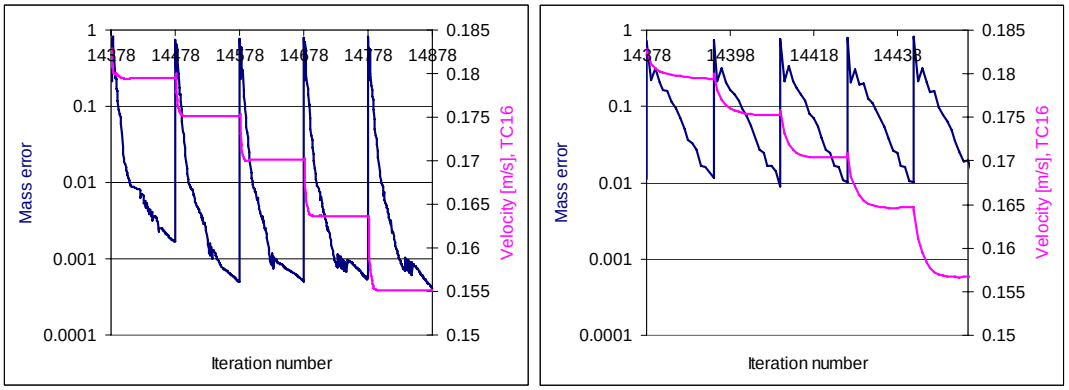

Figure 5. Effect of convergence criterion to flow velocity in TC16 in downcomer: 100 iterations per time step (left) compared to iteration criterion based on the total mass iteration error summed over the mesh (mass residual) < 0.01 (right).

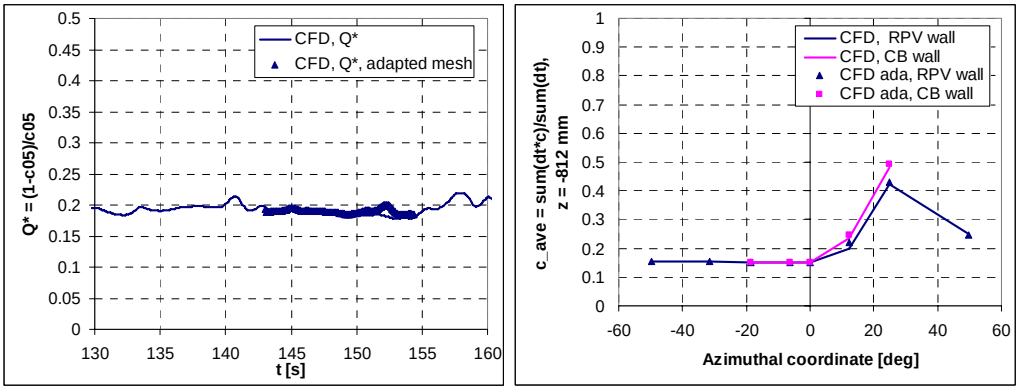

Figure 6. Comparison of selected target variables in simulations with basic mesh and time step size and adapted mesh and halve time step size. *Q (left) and the average concentration values at TC locations 18-25 at the RPV wall and 26-30 at the CB wall at level $z = -821$ mm below the cold leg level (right).**

Simulation of PTS experiment

The basic behavior of flow during the transient was qualitatively similar in calculation and in experiment. There was a local region of mixing in the cold leg around the HPI injection, stratification in the most part of the cold leg with some back flow from the downcomer to the cold leg and a vertical plume in the downcomer that was circumferentially symmetric in the beginning of transient but then "chose" one side of the downcomer. The behavior of the plume in the downcomer near the RPV wall is visualized in Figure 8 at selected times during the transient.

The backflow ratio Q^* presented in Figure 7 is quite similar during the first 160 seconds, after that there is some rapid variation in simulation. The thermocouple location TC05 used in comparison is just at the junction of cold leg and downcomer, and it can be confirmed that the reason for variation is a small "tongue" of cold downcomer water locally interfering the measurement location in the simulation. The backflow ratio computed based on TC55 located further in the cold leg is included to Figure 7 to demonstrate that. The absolute deviation between the simulation and experiment in Q^* can be estimated to be less than 0.1, if this local disturbance is neglected.

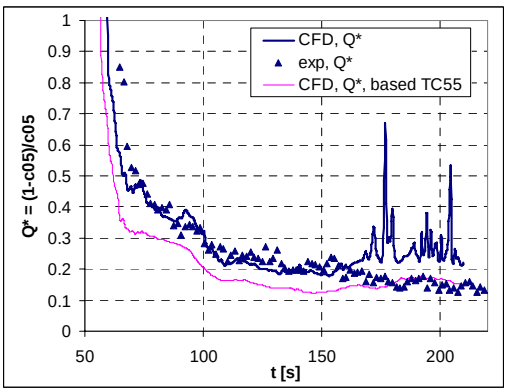

Figure 7. The backflow ratio Q^* as a function of time defined based on TC05 and for CFD simulation also based on TC55.

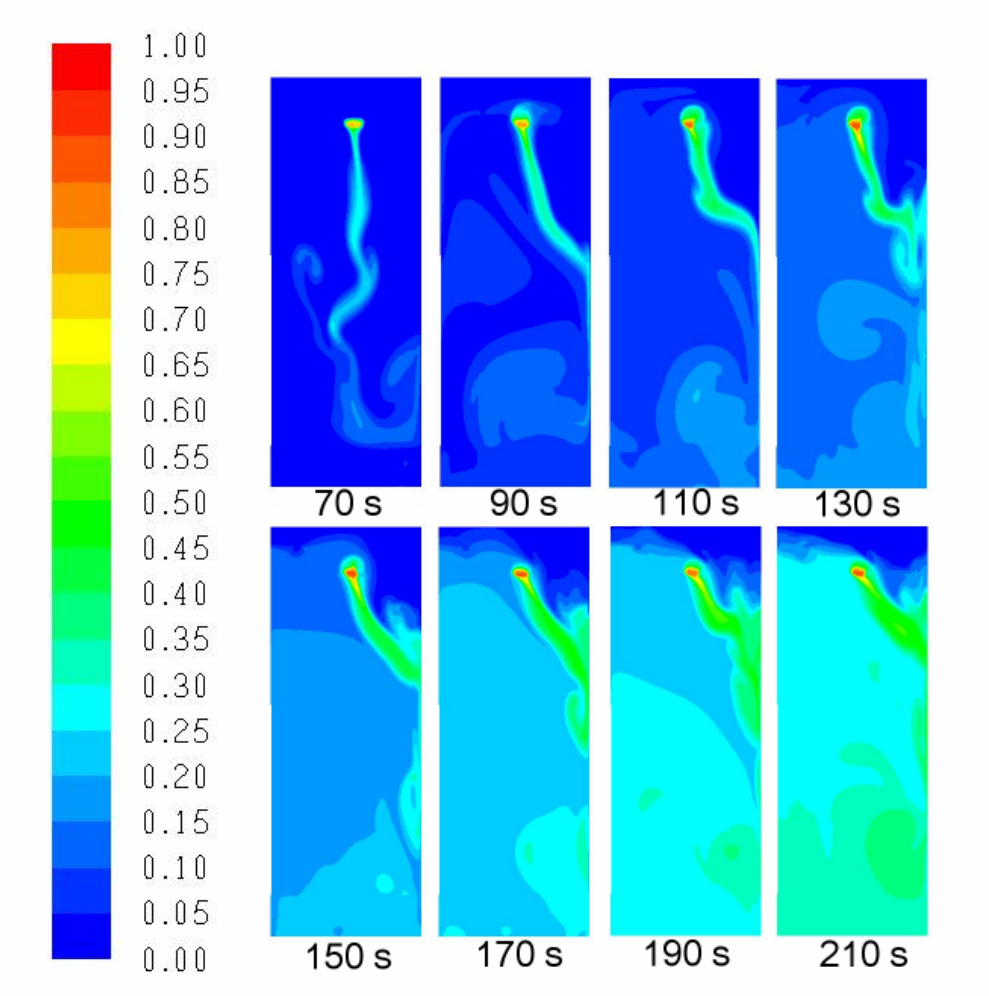

Figure 8. Behavior of the HPI water plume in the downcomer at selected times during the transient. Angle of view from the axis of RPV

The behavior of the cold/salt water plume in the downcomer was estimated calculating average values of concentration in thermocouples at vertical levels $z = -164$ mm, $z = -812$ mm and $z = -1460$ over the total simulation period of about 200 seconds. This target variable is relevant considering the real PTS simulations as it corresponds to the local thermal load to the RPV wall. The first blind comparison of values indicated unsatisfactory equivalence. However when the fact that the cold plume seeks the other circumferential side of the downcomer in CFD simulation than in the experiment, that tendency of cold plume to choose different sides in different experiments had been also confirmed in experiments, is taken into account the comparison gave relatively good results as presented in Figures 9 and 10. At level $z = -164$ mm just below the cold leg the shape of value distribution depends mostly on the mixing in the cold leg, Q^*, and values are quite similar. At level $z = -812$ mm the average value at the side without plume is about 0.11 in CFD simulation and 0.12 in experiment. The average value at the side of the plume is 0.23 in CFD simulation and 0.21 in the experiment. At level $z = -1460$, which is especially interesting in case of Loviisa NPP because of the circumferential weld in the downcomer, the average value at the side without plume is about 0.12 in CFD simulation and 0.13 in experiment. The average value at the side of plume is 0.18 in CFD simulation and 0.17 in experiment.

While there is some difference between the absolute values it can be estimated that stress analyses based on simulation with this accuracy level would give useful best estimates for many applications.

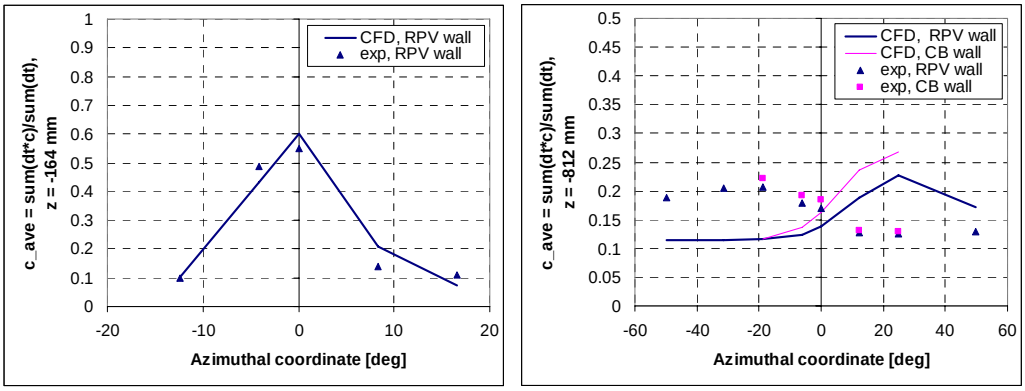

Figure 9. Average concentration over calculation period at TCs near RPV wall: CFD simulation and experiment. Vertical levels *z* = −164 mm (left) and *z* = −812 mm (right) below the cold leg level. At level z=-812 mm also TCs near the core barrel (CB) wall are included to figure.

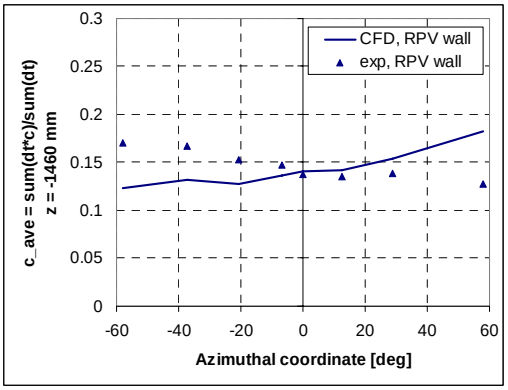

Figure 10 Average concentration over calculation period at TCs at RPV wall: CFD simulation and experiment. Vertical level z = −1460 below the cold leg level.

Comparison of values at level *z*=-812 mm gives some insight also to the radial location of cold HPI plume in the downcomer. Both experimental and calculated values indicate that plume is a little more time near the core barrel wall (CB) than RPV wall at this vertical level. The difference of CB and RPV values at same TCs is larger in CFD simulation, indicating possible a little less mixing of cold plume in CFD simulation. However the small number of TCs prevents to make more comprehensive study.

The experiments did not include velocity measurements. However based on the recorded video in experiment with the same density difference but also with small cold leg flows the vertical velocity of plume about 800 mm below the cold leg nozzle was estimated to be about 0.85 m/s. At CFD simulation the velocity was about 0.6-0.8 m/s, varying depending on the time of the simulation.

Conclusions

The CFD simulation of the Fortum PTS experiment with a commercial CFD code and basic physical models showed that a quite complex flow and mixing scenario with e.g. stratification and density driven flow can be simulated with adequate accuracy for many applications. The basic flow characteristics of the experiment, stratification in the cold leg and formation of density driven plume that mixes in the downcomer, were reproduced in simulation. When the fact that the plume chose one side of the downcomer in the experiment and another in the CFD simulation was taken into account, also the quantitative comparison indicated that the error was small enough to justify the careful use of the computational method in connection with the thermal hydraulic analysis of real PTS problems in NPPs.

The conclusions above are valid for cases with flow boundary conditions similar enough to the experiment simulated here, and it must be noted that the effect of heat transfer between structures and fluid is not taken into account in these simulations. Also it was clear that modeling aspects like convergence and computation mesh are important, for example temporary poor convergence of calculation can lead even to qualitatively wrong flow field.

Nomenclature

c = mass fraction of the HPI water

CLF = Courant, Freidricks, Levy (CFL) number, $\Delta t \times v / \Delta x_{\text{cell}}$

D = (molecular) mass diffusivity

i = index

k = turbulent kinetic energy

I = turbulence intensity u'/u_{avg}

l = turbulence length scale

p = pressure

Q = volumetric flow rate

Sc_{t} = effective Schmidt number

y^+ = wall Y plus, $\rho v_\tau y/\mu$, $v_\tau = (\tau_w/\rho_w)^{1/2}$

Greek letters

ε = turbulent dissipation rate

ρ = density

μ = viscosity

Subscripts

ave = average

inlet = flown inlet of the CFD model

outlet = flow outlet of the CFD model

t = turbulent

Abbreviations

CB = core barrel

CFD = computational fluid dynamics

CL = cold leg

ECCS = emergency core coolant system

HPI = high-pressure safety injection

PTS = pressurized thermal shock

RPV = reactor pressure vessel

TC00 = thermocouple location 00

VVER = Russian PWR type; VVER-440 of 440 MW power

References

[1] "Guidelines on Pressurized Thermal Shock Analysis for WWER Nuclear Power Plants", IAEA document IAEA-EBP-WWER-08, draft (Dec. 2001).

[2] U. Rohde et al., "Validation of CFD Codes Based on Mixing Experiments", FLOMIX-R EU project, final report of work package 4 (2004).

[3] H. Tuomisto, "Thermal-Hydraulics of the Loviisa Reactor Pressure Vessel Overcooling Transient", Fortum research report (1987).

[4] M.Casey et al., "Best Practice Guidelines, version 1.0", ERCOFTAC Special Interest Group on Quality and Trust in Industrial CFD, report (Jan. 2000).

[5] F. Menter et al., "CFD Best Practice Guidelines for CFD code Validation for Reactor Safety Applications", ECORA EU-project, report (2002).

[6] FLUENT 6.2 Documentation, User's Guide, manual (2006).